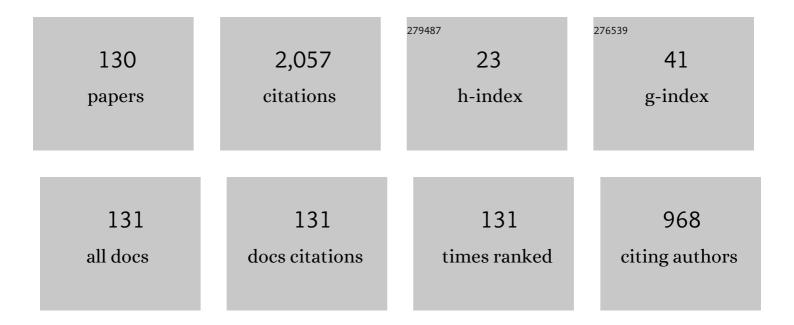
Yoshiaki Mokuno

List of Publications by Year in descending order

Source: https://exaly.com/author-pdf/9000608/publications.pdf Version: 2024-02-01



#	Article	IF	CITATIONS
1	The effect of nitrogen addition during high-rate homoepitaxial growth of diamond by microwave plasma CVD. Diamond and Related Materials, 2004, 13, 1954-1958.	1.8	148
2	Synthesizing single-crystal diamond by repetition of high rate homoepitaxial growth by microwave plasma CVD. Diamond and Related Materials, 2005, 14, 1743-1746.	1.8	107
3	Synthesis of large single crystal diamond plates by high rate homoepitaxial growth using microwave plasma CVD and lift-off process. Diamond and Related Materials, 2008, 17, 415-418.	1.8	107
4	A 2-in. mosaic wafer made of a single-crystal diamond. Applied Physics Letters, 2014, 104, .	1.5	105
5	Fabrication of 1 Inch Mosaic Crystal Diamond Wafers. Applied Physics Express, 2010, 3, 051301.	1.1	86
6	Fabrication and fundamental characterizations of tiled clones of single-crystal diamond with 1-inch size. Diamond and Related Materials, 2012, 24, 29-33.	1.8	75
7	Improving purity and size of single-crystal diamond plates produced by high-rate CVD growth and lift-off process using ion implantation. Diamond and Related Materials, 2009, 18, 1258-1261.	1.8	74
8	Uniform growth and repeatable fabrication of inch-sized wafers of a single-crystal diamond. Diamond and Related Materials, 2013, 33, 27-31.	1.8	59
9	High rate homoepitaxial growth of diamond by microwave plasma CVD with nitrogen addition. Diamond and Related Materials, 2006, 15, 455-459.	1.8	58
10	Characterization of Schottky barrier diodes on a 0.5-inch single-crystalline CVD diamond wafer. Diamond and Related Materials, 2010, 19, 208-212.	1.8	49
11	Damage-free highly efficient polishing of single-crystal diamond wafer by plasma-assisted polishing. CIRP Annals - Manufacturing Technology, 2018, 67, 353-356.	1.7	43
12	Large reduction of threading dislocations in diamond by hot-filament chemical vapor deposition accompanying W incorporations. Applied Physics Letters, 2018, 113, .	1.5	43
13	Characterizations of etch pits formed on single crystal diamond surface using oxygen/hydrogen plasma surface treatment. Diamond and Related Materials, 2016, 63, 43-46.	1.8	42
14	Developments of elemental technologies to produce inch-size single-crystal diamond wafers. Diamond and Related Materials, 2011, 20, 616-619.	1.8	40
15	Simulation of microwave plasmas concentrated on the top surface of a diamond substrate with finite thickness. Diamond and Related Materials, 2006, 15, 1383-1388.	1.8	36
16	Simplified description of microwave plasma discharge for chemical vapor deposition of diamond. Journal of Applied Physics, 2007, 101, 063302.	1.1	36
17	A nitrogen doped low-dislocation density free-standing single crystal diamond plate fabricated by a lift-off process. Applied Physics Letters, 2014, 104, .	1.5	34
18	Room-temperature bonding of single-crystal diamond and Si using Au/Au atomic diffusion bonding in atmospheric air. Microelectronic Engineering, 2018, 195, 68-73.	1.1	34

#	Article	IF	CITATIONS
19	Formation of Crystalline SiC Buried Layer by High-Dose Implantation of MeV Carbon lons at High Temperature. Japanese Journal of Applied Physics, 1993, 32, L1286-L1288.	0.8	32
20	Low resistivity p+ diamond (100) films fabricated by hot-filament chemical vapor deposition. Diamond and Related Materials, 2015, 58, 110-114.	1.8	32
21	Predominant physical quantity dominating macroscopic surface shape of diamond synthesized by microwave plasma CVD. Diamond and Related Materials, 2007, 16, 576-580.	1.8	27
22	Characterization of crystallinity of a large self-standing homoepitaxial diamond film. Diamond and Related Materials, 2009, 18, 216-219.	1.8	25
23	Schottky barrier diodes fabricated on diamond mosaic wafers: Dislocation reduction to mitigate the effect of coalescence boundaries. Applied Physics Letters, 2019, 114, .	1.5	25
24	Preliminary experimental results on mapping of the elemental distribution of the organic tissues surrounding titanium-alloy implants. Nuclear Instruments & Methods in Physics Research B, 1996, 109-110, 278-283.	0.6	23
25	Improvements of crystallinity of single crystal diamond plates produced by lift-off process using ion implantation. Diamond and Related Materials, 2010, 19, 128-130.	1.8	23
26	Toward Highâ€Performance Diamond Electronics: Control and Annihilation of Dislocation Propagation by Metalâ€Assisted Termination. Physica Status Solidi (A) Applications and Materials Science, 2019, 216, 1900498.	0.8	23
27	Simulation of temperature and gas flow distributions in region close to a diamond substrate with finite thickness. Diamond and Related Materials, 2006, 15, 1738-1742.	1.8	21
28	Numerical analyses of a microwave plasma chemical vapor deposition reactor for thick diamond syntheses. Diamond and Related Materials, 2006, 15, 1389-1394.	1.8	20
29	Modeling and numerical analyses of microwave plasmas for optimizations of a reactor design and its operating conditions. Diamond and Related Materials, 2005, 14, 1776-1779.	1.8	19
30	Defect and field-enhancement characterization through electron-beam-induced current analysis. Applied Physics Letters, 2017, 110, .	1.5	19
31	High-resolution X-ray spectroscopy for copper and copper oxides and a new WDX system using an ion microbeam. Nuclear Instruments & Methods in Physics Research B, 2002, 193, 877-882.	0.6	18
32	Numerical analysis of power absorption and gas pressure dependence of microwave plasma using a tractable plasma description. Diamond and Related Materials, 2006, 15, 1395-1399.	1.8	17
33	Numerical microwave plasma discharge study for the growth of large single-crystal diamond. Diamond and Related Materials, 2015, 54, 9-14.	1.8	17
34	Ohmic contact formation to heavily boron-doped p+ diamond prepared by hot-filament chemical vapor deposition. MRS Advances, 2016, 1, 3489-3495.	0.5	17
35	Growth and characterization of freestanding p+ diamond (100) substrates prepared by hot-filament chemical vapor deposition. Diamond and Related Materials, 2018, 81, 33-37.	1.8	17
36	Atomic scale interactions between hydrocarbon radicals and diamond (100) surfaces. Diamond and Related Materials, 2006, 15, 522-525.	1.8	16

#	Article	IF	CITATIONS
37	High energy resolution PIXE with high efficiency using the heavy ion microbeam. Nuclear Instruments & Methods in Physics Research B, 1997, 130, 243-246.	0.6	15
38	Numerical and experimental studies of high growth-rate over area with 1-inch in diameter under moder moderate input-power by using MWPCVD. Diamond and Related Materials, 2008, 17, 1062-1066.	1.8	15
39	Large Single Crystal Diamond Plates Produced by Microwave Plasma CVD. Materials Science Forum, 0, 615-617, 991-994.	0.3	15
40	Method to increase the thickness and quality of diamond layers using plasma chemical vapor deposition under (H, C, N, O) system. Diamond and Related Materials, 2020, 101, 107652.	1.8	15
41	Microprobe PIXE analysis of aluminium in the brains of patients with Alzheimer's disease. Nuclear Instruments & Methods in Physics Research B, 1996, 109-110, 362-367.	0.6	14
42	Crystallinity of freestanding large undoped single crystal diamond plates produced using pre-ion-implanted substrates and lift-off processes. Diamond and Related Materials, 2010, 19, 1259-1262.	1.8	14
43	Effect of Ar addition on uniformity of diamond growth by using microwave plasma chemical vapor deposition. Diamond and Related Materials, 2018, 87, 143-148.	1.8	14
44	WDX-PIXE analysis of low energy X-rays using a microbeam. Nuclear Instruments & Methods in Physics Research B, 1999, 150, 109-113.	0.6	13
45	Chemical state analysis of Cu, Cu2O and CuO with WDX using an ion microbeam. Nuclear Instruments & Methods in Physics Research B, 2001, 181, 128-133.	0.6	13
46	Formation of hydrogenated amorphous carbon films by plasma based ion implantation system applying RF and negative high voltage pulses through single feedthrough. Surface and Coatings Technology, 2002, 156, 328-331.	2.2	13
47	Enhanced annealing of damage in ion-implanted 4H-SiC by MeV ion-beam irradiation. Journal of Applied Physics, 2005, 97, 103538.	1.1	13
48	Fano factor evaluation of diamond detectors for alpha particles. Physica Status Solidi (A) Applications and Materials Science, 2016, 213, 2629-2633.	0.8	13
49	Nitrogen diffusion in stainless steel during irradiation with mass-selected low-energy N+ ion beams. Surface and Coatings Technology, 2005, 196, 271-274.	2.2	12
50	High energy resolution PIXE analysis using focused MeV heavy ion beams. Nuclear Instruments & Methods in Physics Research B, 1998, 136-138, 368-372.	0.6	11
51	Microwave plasma generated in a narrow gap to achieve high power efficiency during diamond growth. Diamond and Related Materials, 2009, 18, 117-120.	1.8	10
52	Configuration of a single grown-in dislocation corresponding to one etch pit formed on the surface of CVD homoepitaxial diamond. Journal of Crystal Growth, 2016, 455, 71-75.	0.7	10
53	Microstructures of threading dislocation bundles included in CVD homoepitaxial diamond plates. Diamond and Related Materials, 2017, 78, 44-48.	1.8	10
54	lon mass dependence of normalized regrowth rate in MeV ion beam induced epitaxial crystallization. Nuclear Instruments & Methods in Physics Research B, 1995, 106, 277-280.	0.6	9

#	Article	IF	CITATIONS
55	Radiation effects of 200 keV and 1 MeV Ni ion on MgO single crystal. Journal of Nuclear Materials, 1999, 271-272, 15-20.	1.3	9
56	Epitaxial Growth of Pure 28Si Thin Films Using Isotopically Purified Ion Beams. Japanese Journal of Applied Physics, 2001, 40, L1283-L1285.	0.8	9
57	Simulation with an improved plasma model utilized to design a new structure of microwave plasma discharge for chemical vapor deposition of diamond crystals. Diamond and Related Materials, 2008, 17, 494-497.	1.8	9
58	Effects of crystallographic orientation on the homoepitaxial overgrowth on tiled single crystal diamond clones. Diamond and Related Materials, 2015, 57, 17-21.	1.8	9
59	Synthesis and characterization of diamond capsules for direct-drive inertial confinement fusion. Diamond and Related Materials, 2018, 86, 15-19.	1.8	9
60	Raman spectra of a cross section of a large single crystal diamond synthesized by using microwave plasma CVD. Diamond and Related Materials, 2010, 19, 171-173.	1.8	8
61	Lifetime and migration length of B-related admolecules on diamond {1 0 0}-surface: Comparative study of hot-filament and microwave plasma-enhanced chemical vapor deposition. Journal of Crystal Growth, 2017, 479, 52-58.	0.7	8
62	PIXE analysis of trace elements in northern fur seal teeth. Nuclear Instruments & Methods in Physics Research B, 1999, 150, 267-271.	0.6	7
63	Qualitative Correspondences of Experimentally Obtained Growth Rates and Morphology of Single-Crystal Diamond with Numerical Predictions of Plasma and Gas Dynamics in Microwave Discharges for Various Substrate Holder Shapes. Japanese Journal of Applied Physics, 2006, 45, 8177-8182.	0.8	7
64	Development of single-crystalline diamond wafers. Synthesiology, 2010, 3, 272-280.	0.2	7
65	Fast removal of surface damage layer from single crystal diamond by using chemical etching in molten KCl + KOH solution. Diamond and Related Materials, 2016, 63, 86-90.	1.8	7
66	Heat and radiation resistances of diamond semiconductor in gamma-ray detection. Japanese Journal of Applied Physics, 2019, 58, 106509.	0.8	7
67	Model of Reactive Microwave Plasma Discharge for Growth of Single-Crystal Diamond. Japanese Journal of Applied Physics, 2011, 50, 01AB02.	0.8	7
68	Damage of polyimide thin films irradiated by MeV proton microbeams. Nuclear Instruments & Methods in Physics Research B, 1995, 104, 55-58.	0.6	6
69	Development of single-crystalline diamond wafers. Synthesiology, 2010, 3, 259-267.	0.2	6
70	Model of Reactive Microwave Plasma Discharge for Growth of Single-Crystal Diamond. Japanese Journal of Applied Physics, 2011, 50, 01AB02.	0.8	6
71	Diamond slicing using ultrashort laser-induced graphitization and additional nanosecond laser illumination. Diamond and Related Materials, 2019, 96, 126-133.	1.8	6
72	Observation of local SIMOX layers by microprobe RBS. Nuclear Instruments & Methods in Physics Research B, 1994, 85, 921-924.	0.6	5

#	Article	IF	CITATIONS
73	Properties of diamond like carbon films by plasma based ion implantation and deposition method applying radio frequency wave and negative high voltage pulses through single feedthrough. Nuclear Instruments & Methods in Physics Research B, 2003, 206, 717-720.	0.6	5
74	Metal plasma source for PBII using arc-like discharge with hot cathode. Surface and Coatings Technology, 2004, 186, 157-160.	2.2	5
75	Characterization of a sandwich-type large CVD single crystal diamond particle detector fabricated using a lift-off method. Diamond and Related Materials, 2012, 24, 74-77.	1.8	5
76	Submicron-scale diamond selective-area growth by hot-filament chemical vapor deposition. Thin Solid Films, 2016, 615, 239-242.	0.8	5
77	Characterization of X-ray radiation hardness of diamond Schottky barrier diode and metal-semiconductor field-effect transistor. , 2017, , .		5
78	MeV heavy ion microprobe PIXE for the analysis of the materials surface. Nuclear Instruments & Methods in Physics Research B, 1994, 85, 741-743.	0.6	4
79	L X-ray spectra of Fe and Cu by 0.75 MeV/u H, He, Si and Ar ion impacts. Nuclear Instruments & Methods in Physics Research B, 1996, 107, 47-50.	0.6	4
80	<title>Correlation filter design for classification of road sign by multiple optical correlators</title> . , 1999, , .		4
81	Ion-Beam 3C–SiC Heteroepitaxy on Si. Japanese Journal of Applied Physics, 2002, 41, 7353-7354.	0.8	4
82	3C-SiC thin epilayer formation at low temperature using ion beams. Applied Surface Science, 2003, 212-213, 920-925.	3.1	4
83	Freestanding single crystal chemical vapor deposited diamond films produced using a lift-off method: Response to α-particles from 241Am and crystallinity. Nuclear Instruments & Methods in Physics Research B, 2012, 286, 313-317.	0.6	4
84	Lattice structure of a freestanding nitrogen doped large single crystal diamond plate fabricated using the lift-off process: X-ray diffraction studies. Diamond and Related Materials, 2012, 25, 119-123.	1.8	4
85	Short-pulse excitation of microwave plasma for efficient diamond growth. Applied Physics Letters, 2016, 109, .	1.5	4
86	Doping-induced strain in heavily B-doped (100) diamond films prepared by hot-filament chemical vapor deposition. Thin Solid Films, 2019, 680, 85-88.	0.8	4
87	High energy Ni ion implantation and thermal annealing for α-SiC single crystal. Nuclear Instruments & Methods in Physics Research B, 1994, 91, 529-533.	0.6	3
88	Analysis of radiation-induced segregation in type 304 stainless steel by PIXE and RBS channeling. Nuclear Instruments & Methods in Physics Research B, 1996, 118, 363-366.	0.6	3
89	Energy straggling induced errors in heavy-ion PIXE analysis. Nuclear Instruments & Methods in Physics Research B, 1998, 136-138, 179-183.	0.6	3
90	Radiation-induced amorphization and recrystallization of α-SiC single crystal. Journal of Nuclear Materials, 1999, 271-272, 11-14.	1.3	3

#	Article	IF	CITATIONS
91	Sequential implantation of halogen and copper ions in silica glass. Nuclear Instruments & Methods in Physics Research B, 2003, 206, 353-356.	0.6	3
92	In situ monitoring of polyimide windows for external ion microbeams. Nuclear Instruments & Methods in Physics Research B, 2003, 210, 75-78.	0.6	3
93	Investigation of electrically-active deep levels in single-crystalline diamond by particle-induced charge transient spectroscopy. Nuclear Instruments & Methods in Physics Research B, 2016, 372, 151-155.	0.6	3
94	Characterization of insulated-gate bipolar transistor temperature on insulating, heat-spreading polycrystalline diamond substrate. Japanese Journal of Applied Physics, 2017, 56, 011301.	0.8	3
95	A heavy ion microprobe and its application to multi-dimensional processing and analysis. Nuclear Instruments & Methods in Physics Research B, 1993, 79, 424-427.	0.6	2
96	lon monitoring of ion beam dynamic mixing process. Nuclear Instruments & Methods in Physics Research B, 1993, 80-81, 124-127.	0.6	2
97	Characterization of single crystal of type 304 stainless steels using RBS- and PIXE-channeling. Journal of Nuclear Materials, 1995, 223, 210-212.	1.3	2
98	Application of a MeV nickel ion beam for PIXE analysis of iron near the surface of a silicon wafer. Nuclear Instruments & Methods in Physics Research B, 1995, 100, 122-124.	0.6	2
99	Analysis of iron by PIXE using heavy ion microprobes. Nuclear Instruments & Methods in Physics Research B, 1995, 104, 49-51.	0.6	2
100	PIXE analysis of heavy elements in silicon using MeV heavy ion beams. Nuclear Instruments & Methods in Physics Research B, 1996, 109-110, 573-575.	0.6	2
101	Reflection high-energy electron diffraction study of ion-beam induced carbonization for 3C–SiC heteroepitaxial growth on Si (100). Journal of Vacuum Science and Technology A: Vacuum, Surfaces and Films, 2001, 19, 1882-1886.	0.9	2
102	Isotopically-Purified Si and 3C-SiC Film Growth by an Ion-Beam Deposition Method. Physica Status Solidi A, 2002, 189, 169-174.	1.7	2
103	Neutron-enhanced annealing of radiation damage formed by self-ion implantation in silicon. Applied Physics Letters, 2006, 88, 241921.	1.5	2
104	Measurement of charge carrier's transportation in a large size self-standing CVD single crystal diamond film fabricated using lift-off method. Diamond and Related Materials, 2010, 19, 162-165.	1.8	2
105	Neutron-enhanced annealing of ion-implantation induced damage in silicon heated by nuclear reactions. Nuclear Instruments & Methods in Physics Research B, 2014, 334, 48-51.	0.6	2
106	Substrate Effects on Charge Carrier Transport Properties of Singleâ€Crystal CVD Diamonds and an 8 mm Square Radiation Energy Spectrometer. Physica Status Solidi (A) Applications and Materials Science, 2018, 215, 1800333.	0.8	2
107	Dependences of morphology and surface roughness on growth conditions of diamond capsules for the direct-drive inertial confinement fusion. High Energy Density Physics, 2020, 37, 100849.	0.4	2
108	Coaxial Evaporation Source Using Vacuum Arc Discharge Shinku/Journal of the Vacuum Society of Japan, 1997, 40, 300-302.	0.2	2

#	Article	IF	CITATIONS
109	Erosion of Titanium Nitride Coatings Hyomen Gijutsu/Journal of the Surface Finishing Society of Japan, 1992, 43, 1237-1238.	0.1	1
110	Heavy ion microprobe for PIXE analysis of iron. Nuclear Instruments and Methods in Physics Research, Section A: Accelerators, Spectrometers, Detectors and Associated Equipment, 1994, 353, 619-622.	0.7	1
111	Three-dimensional analysis of locally deposited silicon oxide on ferrite by a combination of microprobe RBS and PIXE. Nuclear Instruments & Methods in Physics Research B, 1994, 85, 689-692.	0.6	1
112	Application of chemical effects in X-ray spectra for characterization of the high-Tc superconductors. Applied Superconductivity, 1997, 5, 93-99.	0.5	1
113	Characteristics of Diamond SBD's Fabricated on Half Inch Size CVD Wafer Made by the "Direct Wafer Fabrication Technique― Materials Science Forum, 2010, 645-648, 1227-1230.	0.3	1
114	Surface stress measurement with interference microscopy of thick homoepitaxial single-crystal diamond layers. Diamond and Related Materials, 2010, 19, 1453-1456.	1.8	1
115	Atomic force microscopy observations of a single crystal diamond surface lifted-off via ion implantation. Diamond and Related Materials, 2013, 31, 6-9.	1.8	1
116	Recent progresses in R&D of methods to fabricate inch-sized diamond wafers. , 2014, , 97-106.		1
117	Microanalysis of masklessly MeV-ion-implanted area by MeV heavy-ion microprobe. Nuclear Instruments & Methods in Physics Research B, 1992, 64, 358-361.	0.6	0
118	Maskless fabrication of contact vias by focused MeV heavy ion beam. Nuclear Instruments & Methods in Physics Research B, 1993, 80-81, 1292-1295.	0.6	0
119	Radiation damage and radiation-induced segregation in single crystal stainless steel by RBS and PIXE channeling. Journal of Nuclear Materials, 1999, 271-272, 21-25.	1.3	0
120	High-energy resolution PIXE study of heat induced changes in cadmium compounds using ion microbeam. Nuclear Instruments & Methods in Physics Research B, 1999, 158, 241-244.	0.6	0
121	<title>Diffractive phase element for reducing the diameter of the main lobe of a focal spot</title> . , 2000, , .		0
122	Diffractive phase element for shrinking focal spot diameter: Design, fabrication, and application to laser beam lithography. Optical Review, 2001, 8, 416.	1.2	0
123	Reaction Mechanism of the Carbonization Process by Low-Energy Ion Subplantation. Materials Science Forum, 2002, 389-393, 363-366.	0.3	0
124	Thermal conductivity measurement of diamond and β-Ga <inf>2</inf> O <inf>3</inf> thin films by a 3ω method. , 2018, , .		0
125	Electric Field Characterization of Diamond Metal Semiconductor Field Effect Transistors Using Electron Beam Induced Current. Materials Science Forum, 2018, 924, 935-938.	0.3	0
126	Title is missing!. Shinku/Journal of the Vacuum Society of Japan, 2000, 43, 1036-1041.	0.2	0

#	Article	IF	CITATIONS
127	Nitriding of Vanadium Films by Ion Implantation Shinku/Journal of the Vacuum Society of Japan, 1992, 35, 364-367.	0.2	0
128	Formation of Buried SiC by High-Dose MeV Ion Implantation at High Temperature Shinku/Journal of the Vacuum Society of Japan, 1993, 36, 856-861.	0.2	0
129	Heavy ion microprobes for microanalysis of materials surfaces. , 1994, , 407-411.		0
130	Oxygen Concentration Dependence in Microwave Plasmaâ€Enhanced Chemical Vapor Deposition Diamond Growth in the (H, C, O, N) System. Physica Status Solidi (A) Applications and Materials Science, 0, , 2100887.	0.8	0